Evaluation of the causes of inundation in a repeatedly flooded zone in the city of Cheongju, Korea, using a 1D/2D model

In-Hyeok Park, Jeong-Yong Lee, Ji-Heon Lee and Sung-Ryong Ha

ABSTRACT

Currently, unprecedented levels of damage arising from major weather events have been experienced in a number of major cities worldwide. Furthermore, the frequency and the scale of these disasters appear to be increasing and this is viewed by some as tangible proof of climate change. In the urbanized areas sewer overflows and resulting inundation are attributed to the conversion of previous surfaces into impervious surfaces, resulting in increased volumes of runoff which exceed the capacity of sewer systems and in particular combined sewer systems. In this study, the characteristics of sewer overflows and inundation have been analyzed in a repeatedly flooded zone in the city of Cheongju in Korea. This included an assessment of inundation in a 50-year storm event with total rainfall of 165 mm. A detailed XP-SWMM 2D model was assembled and run to simulate the interaction of the sewerage system overflows and surface inundation to determine if inundation is due to hydraulic capacity limitations in the sewers or limitations in surface inlet capacities or a combination of both. Calibration was undertaken using observation at three locations (PT #1, PT #2, PT #3) within the study area. In the case of the subsurface flow calibration, R^2 value of 0.91 and 0.78 respectively were achieved at PT #1 and PT #2. Extremely good agreement between observed and predicted surface flow depths was achieved also at PT #1 and PT #2. However, at PT #3 the predicted flow depth was 4 cm lower than the observed depth, which was attributed to the impact of buildings on the local flow distribution. Areas subject to flooding were classified as either Type A (due to insufficient hydraulic capacity of a sewer), Type B (which is an area without flooding notwithstanding insufficient hydraulic capacity of a sewer) or Type C (due to inlet limitations, i.e. there is hydraulic capacity in a sewer which is not utilized). In the total flooded zone, 24% was classified as Type A (10.2 ha) and 25% was classified as Type C (2.61 ha). It was concluded that greater attention should be paid to the area classified as Type B, which covers 50.5% (5.15 ha) of the total flooded zone.

Key words | 1D/2D model, dual drainage, inundation, sewer overflows

In-Hyeok Park
Jeong-Yong Lee
Ji-Heon Lee
Sung-Ryong Ha (corresponding author)
Department of Urban Engineering,
Chungbuk National University,
Cheongju,
South Korea
E-mail: *simplet@chungbuk.ac.kr*

INTRODUCTION

Currently, unprecedented levels of damage arising from major weather events have been experienced in a number of major cities worldwide. Furthermore, the frequency and the scale of these disasters appear to be increasing and this is viewed by some as tangible proof of climate change. In the urbanized areas sewer overflows and resulting inundation are attributed to the conversion of previous surfaces into impervious surfaces, resulting in increased volumes of runoff which exceed the capacity of sewer systems and in particular combined sewer systems.

Recent studies on the effect of inundation and on the hydrologic response have examined the impact of urban drainage on flooding in terms of the drainage network structure (Meierdiercks *et al.* 2010), drainage network efficiency (Aronica &

doi: 10.2166/wst.2014.077

Lanza 2005), drainage pathway distribution (Leitao *et al.* 2009) and model resolution (Fewtrell *et al.* 2008; Schubert *et al.* 2008).

This study is focused on assembling and running a 1D/2D model to assess the sewer carrying capacity and the inundation resulting from overflows and potential re-capture of these surface flows elsewhere in the sewerage system in a study area within the city of Cheongju, Korea.

MATERIALS AND METHODS

Overview of the study area

The study area is a frequently flooded area in the city of Cheongju which is located in the Chungcheongbuk Province of South Korea. The study area is located on the right bank of the Moosim River which flows through Cheongju. The Moosim River has its headwaters on the Wooam Mountain (elevation 343 m). Outside the mountainous terrain, the average elevation of the study area varies from a minimum 38.15 m to a maximum 42.5 m.

Figure 1 shows the study area, which is a typical residential area, mostly composed of detached housing and the centre district which houses commercial facilities. The total length of the sewer system in the study area is 18.1 km and the average sewer size is approximately 700 mm in diameter. The study area is 96% impervious and the total basin area is 1,184 ha. The terrain was represented using a DSM (digital surface model) created from LiDAR data. A bilinear interpolation method was applied to transform the DSM dataset from 1 m × 1 m dataset into 5 m × 5 m dataset.

Overview of the dual-drainage system model

The concept of a dual-drainage system, proposed by Djordjevic *et al.* (1999), is implemented by assembling a 1D model of both the subsurface system which is linked to a 2D model of surface overland flow paths. This overcomes the problem experienced in a simpler 1D urban flooding model where any surcharge flows are held at a manhole until the capacity of the system recovers and is able to drain away stored flow. In this study, an XP-SWMM 2D model was

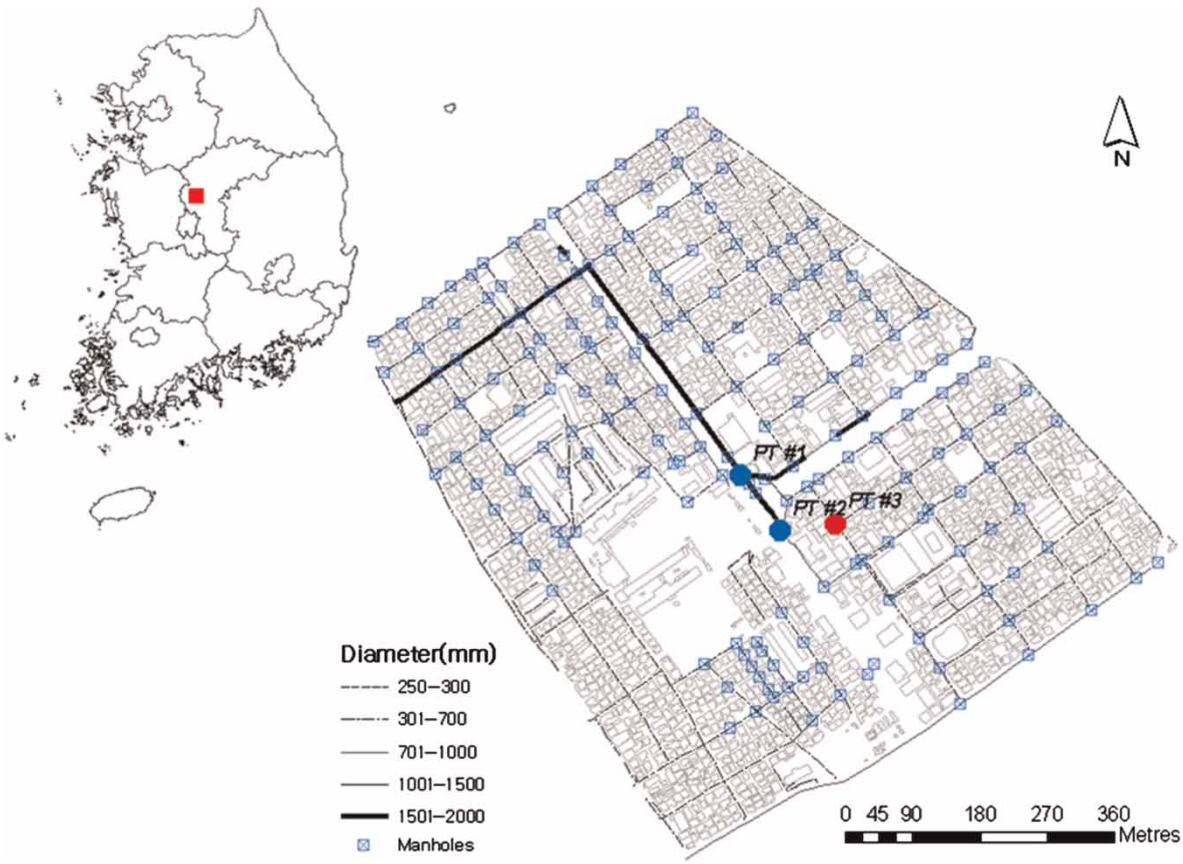

Figure 1 | Study area.

selected to simulate the interaction of the sewerage system overflows and resulting surface inundation. XP-SWMM 2D is a modelling system which couples the 1D SWMM (Storm Water Management Model) algorithms developed by the US Environmental Protection Agency (USEPA) and the 2D TUFLOW algorithm developed by WBM Oceanics (2003).

The governing equations of subsurface flow (in the form of 1D unsteady gradually varied flow equations) are (Lai 1986)

$$\frac{\partial A}{\partial t}+\frac{\partial Q}{\partial s}-q_1+q_2=0 \tag{1}$$

$$\frac{\partial Q}{\partial t}+\frac{\partial}{\partial s}\left(\frac{Q^2}{A}\right)-\mathrm{g}A\left(S_0-\frac{\partial d}{\partial s}-S_f\right)+q_2\left(\frac{Q}{A}\right)=0 \tag{2}$$

where A and Q are the cross-sectional area and discharge of the channel, respectively; q_1 is the lateral inflow per unit length flowing from the floodplain to the channel; q_2 is the lateral outflow per unit length flowing from the channel to the floodplain; s is the coordinate in the longitudinal direction; g is gravitational acceleration; S_0 is the bed slope; d is the flow depth and S_f is the friction slope.

The governing equations of surface flow (inundation) are

$$\frac{\partial \mathbb{C}}{\partial t}+\frac{\partial(Hu)}{\partial x}+\frac{\partial(H\gamma)}{\partial y}=0 \tag{3}$$

$$\frac{\partial u}{\partial t}+u\frac{\partial u}{\partial x}+\gamma\frac{\partial u}{\partial y}-c_f\gamma+g\frac{\partial \mathbb{C}}{\partial x}+gu\left(\frac{n^2}{H^{4/3}}+\frac{f_l}{2g\partial x}\right)\sqrt{u^2+\gamma^2}-\mu\left(\frac{\partial^2 u}{\partial x^2}+\frac{\partial^2 u}{\partial y^2}\right)+\frac{1}{\rho}\frac{\partial P}{\partial x}=F_x \tag{4}$$

$$\frac{\partial \gamma}{\partial t}+u\frac{\partial \gamma}{\partial x}+\gamma\frac{\partial \gamma}{\partial y}-c_f u+g\frac{\partial \mathbb{C}}{\partial y}+g\gamma\left(\frac{n^2}{H^{4/3}}+\frac{f_l}{2g\partial y}\right)\sqrt{u^2+\gamma^2}-\mu\left(\frac{\partial^2 \gamma}{\partial x^2}+\frac{\partial^2 \gamma}{\partial y^2}\right)+\frac{1}{\rho}\frac{\partial P}{\partial y}=F_y \tag{5}$$

where, $\mathbb{C}$ is the water elevation, u is the mean velocity in the X direction, γ is the mean velocity in the Y direction, H is the depth, t is the time, x is the length in the X direction, y is the length in the Y direction, c_f is the Coriolis force coefficient, n is Manning's roughness value, f_l is the form loss coefficient, μ is the momentum horizontal dispersion coefficient, P is the atmospheric pressure, ρ is the density of water, F_x and F_y are each the total sum of external forces in the X and Y directions respectively.

A pre-2009 method offered by an XP-SWMM 2D was selected to simulate the capture of surface flow at an inlet/manhole as follows:

$$Q=A\times(d-h)/t \tag{6}$$

where, A is the catchment area of a manhole, d is the 2-dimensional depth, h is the altitude of a manhole, t is the time interval of simulation.

In this study, contrary to conventional model set-up practice, which considers a limited number of manholes according to a HRU (Hydraulic Response Unit) delineation, all 198 manholes located within the study area were included in the model.

RESULTS AND DISCUSSION

Model calibration

While the aim was to calibrate and validate the 1D (subsurface) and 2D (surface) flows together, observed data were only available separately for subsurface and surface flows. The subsurface model was calibrated using subsurface flow measurements collected only on October 22, 2012. The total rainfall for this event was 37.5 mm with a rainfall intensity of 3.4 mm/hr. The surface flow model was validated using surface measurements collected on October 15, 2012. The total rainfall for this event was 165 mm with a rainfall intensity of 16.5 mm/hr, which is around a 50-year flood event.

Figure 2 shows calibration results of subsurface flow at two sites (PT #1 and PT #2) while inundation depths were recorded at all three sites (PT #1, PT #2, PT #3) to validate the surface flow model. Because there was no CCTV installed to verify the inundation depths, the observed data were acquired from camcorder data during 8 minutes shooting time (17:38–17:46).

A comparison of the observed and predicted subsurface flows and surface flow depths is given in Table 1. In the case of the subsurface flow calibration, R^2 values of 0.91 and 0.78 respectively were achieved at PT #1 and PT #2. In the case of PT #1, a high model reproductive capacity has been achieved with a root-mean-square error (RMSE) value of 0.066 m^3/s. However, in the case of PT #2, a relatively high RMSE value of 1.407 m^3/s was calculated. This was attributed to a difficult base flow simulation due to large inflows from the outskirts of the site in the relatively small basin area.

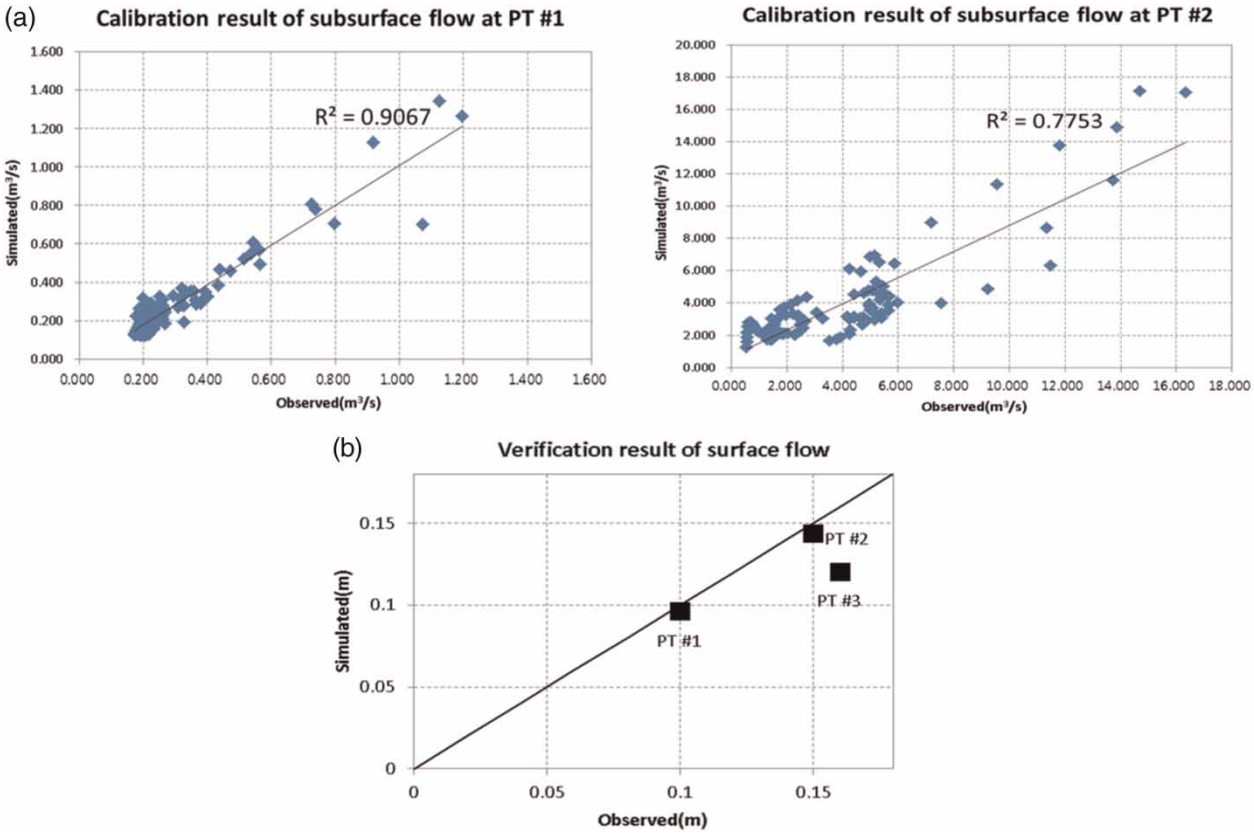

Figure 2 | Subsurface calibration results and surface flow validation results. (a) Subsurface flow calibration (October 22, 2012), (b) surface flow validation (October 15, 2012).

Table 1 | Comparison of observed and predicted subsurface flows and surface flow depths

Variable		PT #1	PT #2	PT #3
Subsurface flow (m^3/s)	Min (Obs./Pred.)	0.174/0.123	0.547/1.23	Not observed
	Max (Obs./Pred.)	1.196/1.34	16.34/17.11	Not observed
	Ave (Obs./Pred.)	0.293/0.276	3.73/3.73	Not observed
	RMSE/R^2	0.066/0.91	1.407/0.78	Not observed
Surface flow depth (m)	Pred.	0.10	0.15	0.12
	Obs.	0.10	0.16	0.16
	RMSE	0.0196		

As shown in Table 1, extremely good agreement between observed and predicted flow depths was achieved at PT #1 and PT #2. However, at PT #3 the predicted flow depth was 4 cm lower than the observed depth, which was attributed to the impact of buildings on the local flow distribution.

The correlations between sewer capacity and inundation

Figure 3 shows the predicted inundation and surface flow velocities at 17:45 on October 15, 2012. The spatial variation in sewer capacity and water head and depth at each manhole at 17:45 h is depicted in Figure 4. The total head of each manhole reflects the elevation in the study area being higher in the east and lower in the west (see Figure 4(a)). The sewer transport pathway is plotted in Figure 4(b). Figure 4(c) plots the spare head at a manhole, which can be up to 40 cm at some locations. This also indicates that inundation of the main road has been caused by inlet limitations not the hydraulic capacity of the sewer system in the flooded zone. More obvious results can be found from the overlapping analysis between the spare

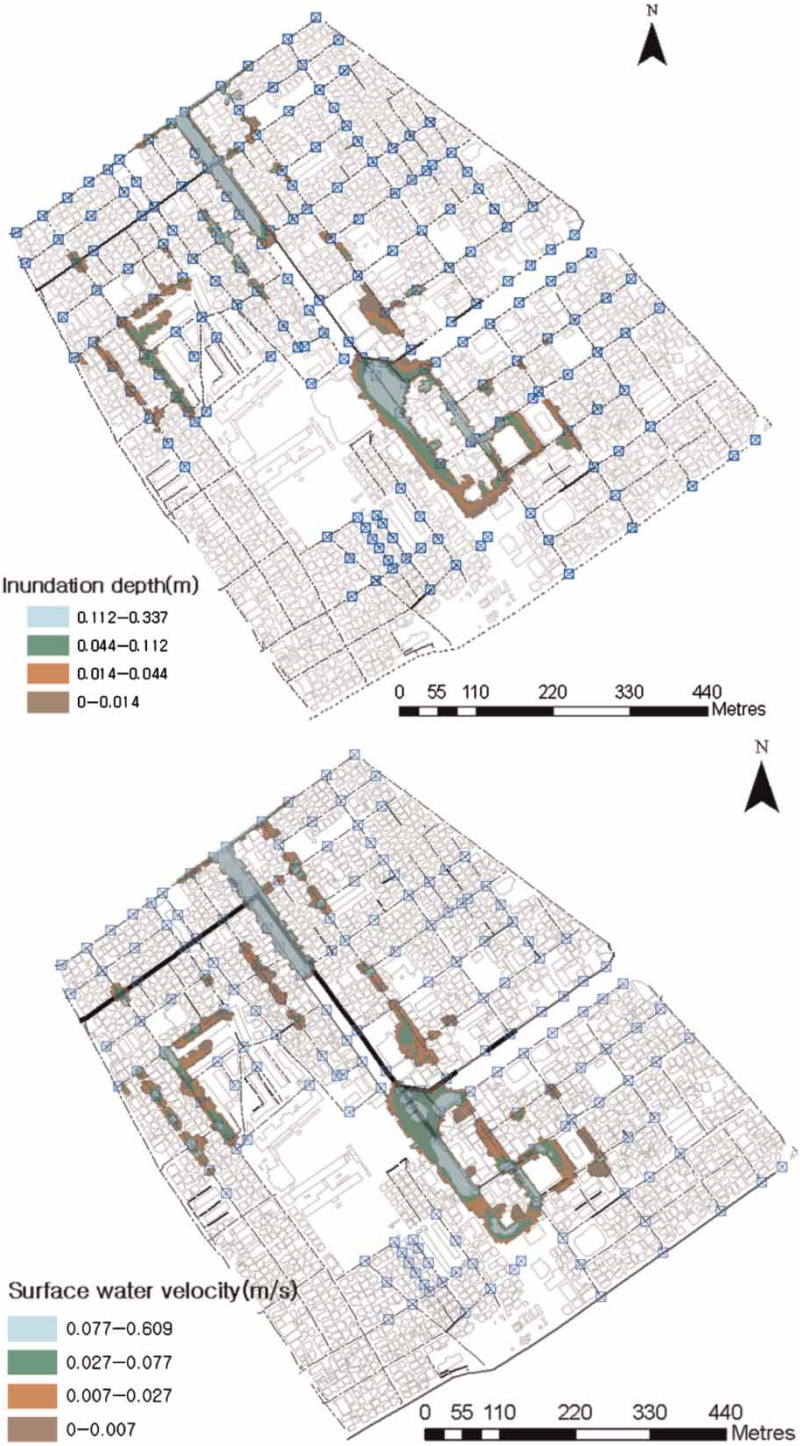

Figure 3 | Inundation depth (m) and flow velocity (m/s) at 17:45 on October 15, 2012.

head at a manhole and the flooded zone. Figure 4(d) shows the resulting classification of flooding. Type A is flooding due to insufficient hydraulic capacity of a sewer, Type B is an area without flooding notwithstanding insufficient hydraulic capacity of a sewer and Type C is flooding due to inlet limitations (i.e. there is hydraulic capacity in a sewer which is not utilized). In the total flooded zone, 24% was classified as Type A (10.2 ha) and 25% was

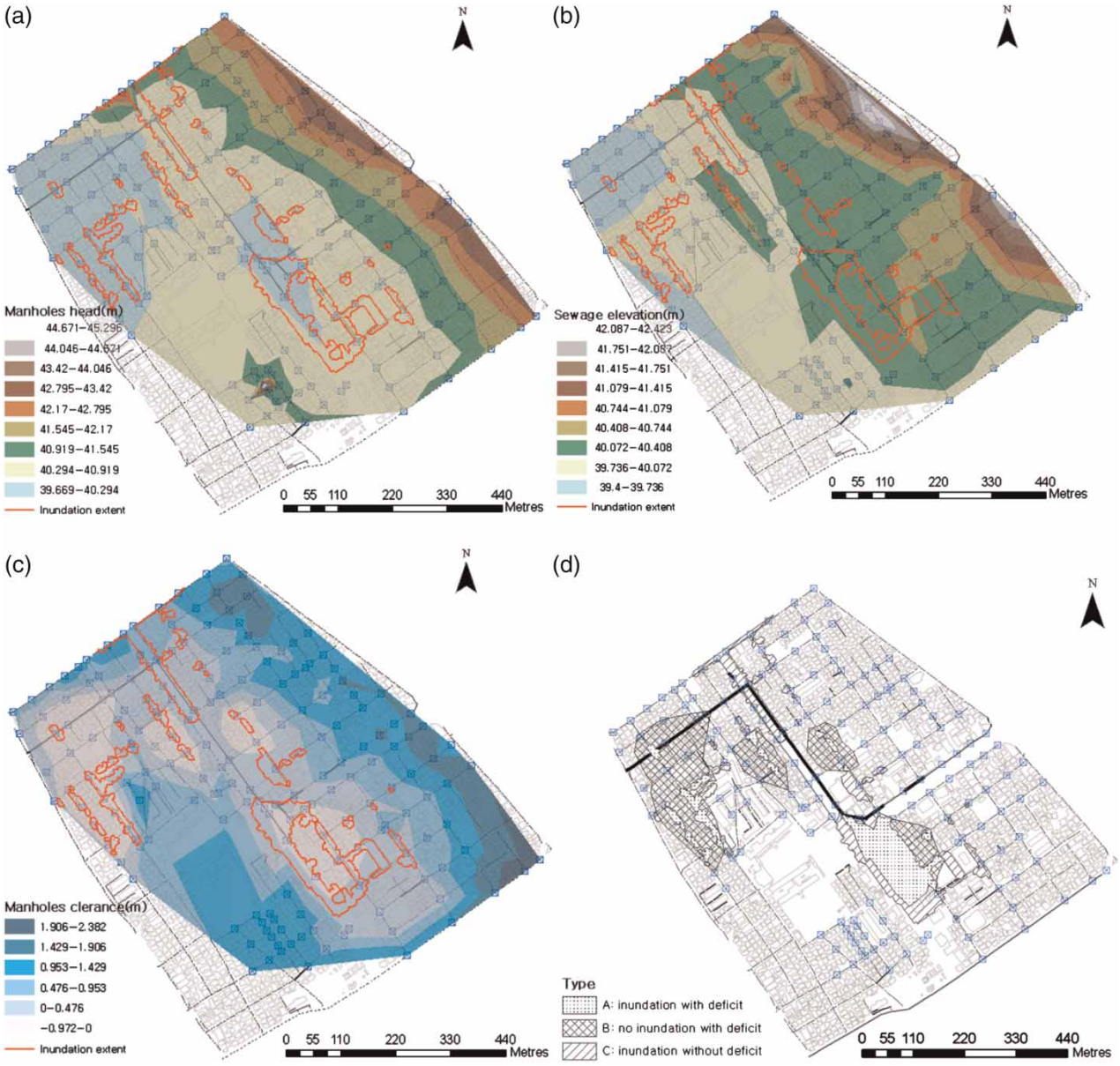

Figure 4 | Schematic contour plots of manhole head, sewage elevation, manhole clearance and inundation type. (a) Manhole head, (b) sewage elevation, (c) manhole clearance, (d) inundation type.

classified as Type C (2.61 ha). More attention should be paid to the area classified as Type B, which covers 50.5% (5.15 ha) of the total flooded zone.

To analyze this mechanism more thoroughly, Figure 5 presents an analysis of the time series change in the water level in the manhole and the head at PT #1 and PT #3. A typical inundation occurrence based on the conventional theoretical backgrounds has been shown on the site of PT #3, which is located in the manhole on a branch sewer line. When overflow commences, the head of surface flow increases and when it has finished overflowing, the head of surface flow decreased suddenly and inundation disappears. However, on the site of PT #1 at the manhole on the main sewer, surface runoff has increased with the start of the overflowing of subsurface component, but after overflowing, the head of surface flow decreases gently compared to the case of PT #3.

Sewer discharge capacity limitations

In the study area, the deficient carrying capacity of the sewer line initiates overflows from the sewer system. This is

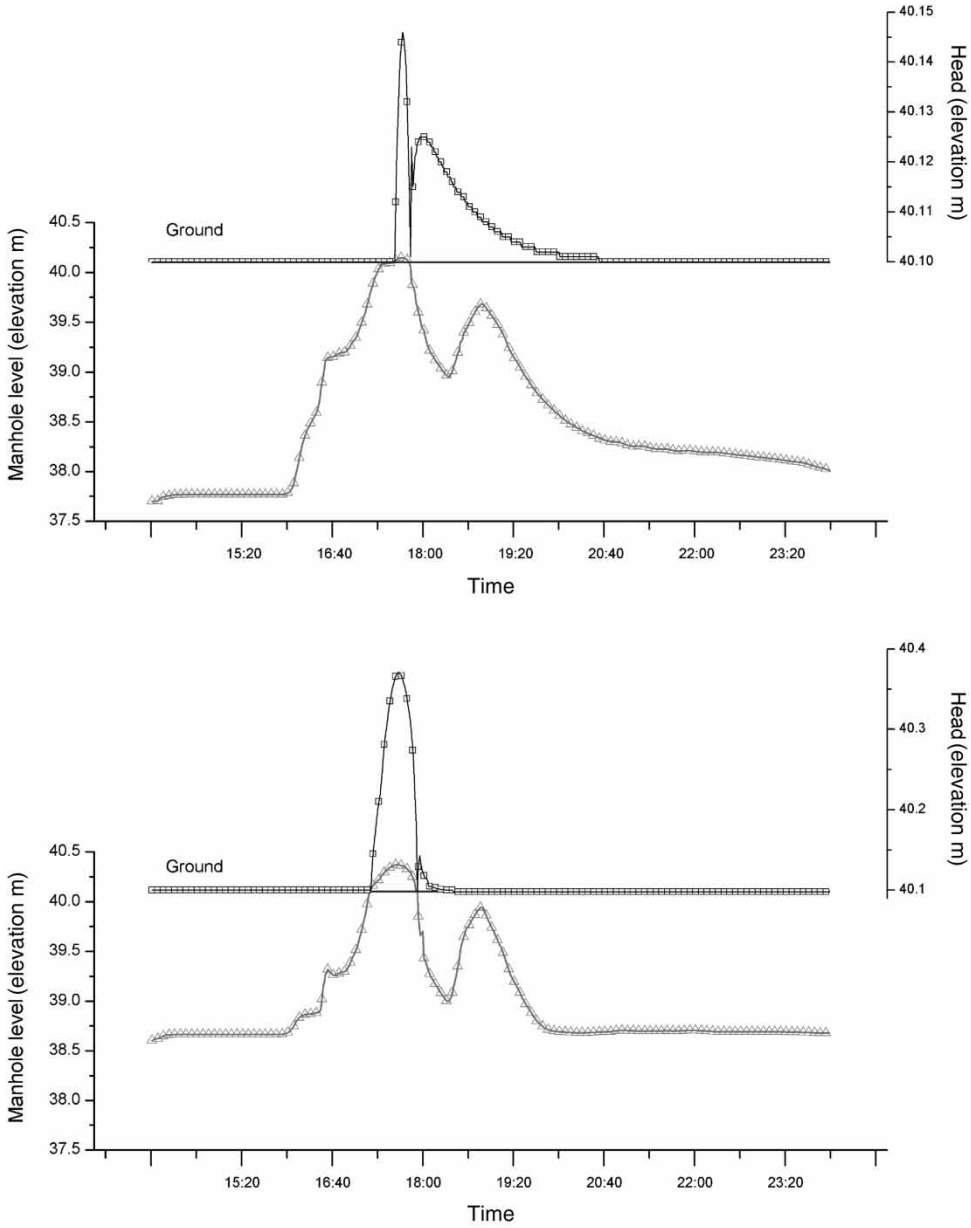

Figure 5 | Hydrograph of water level and head at manholes PT #1 (top) and PT #3 (bottom) (October 15, 2012).

demonstrated in Figure 6 that plots the distribution of the resulting sewer overflows in a branch sewer line in the upper basin.

The results show that 32% of the manholes (64 of 198 sites) overflowed and 64% of the overflowing manholes (15 of 64) surcharged more than 150 m^3. The average overflow volume was 62 m^3 with a maximum volume of 404 m^3. As depicted in Figure 6, District A in the south-east area is highly prone to overflows due to insufficient infrastructure.

In contrast only one site on the trunk sewer overflowed, with the total volume of overflow of only 2 m^3.

CONCLUSIONS

In this research, the characteristics of sewer overflows and inundation have been analyzed in a repeatedly flooded zone in the city of Cheongju in Korea. This included an

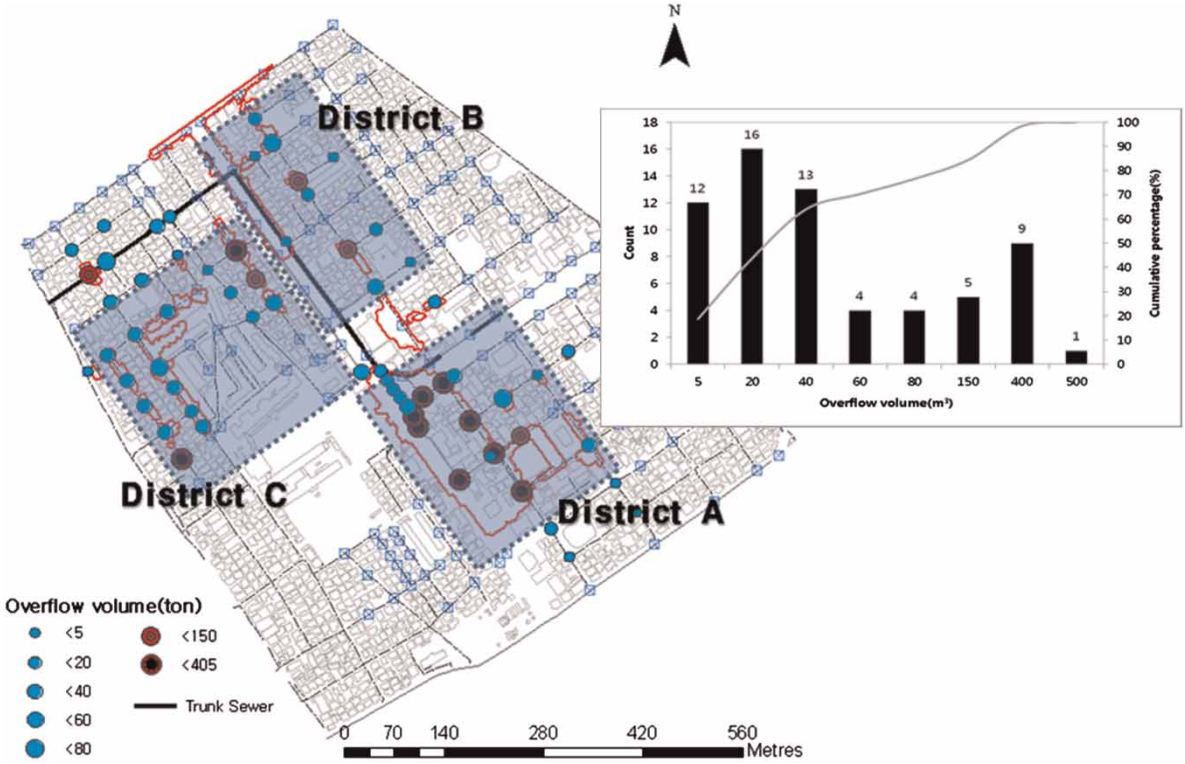

Figure 6 | Map of manholes that overflow and a histogram of overflow volume (m^3).

assessment of inundation in a 50-year storm event with total rainfall of 165 mm.

Calibration was undertaken using observation at three locations within the study area. In the case of the subsurface flow calibration, R^2 values of 0.91 and 0.78 respectively were achieved at PT #1 and PT #2. Extremely good agreement between observed and predicted surface flow depths was achieved also at PT #1 and PT #2. However, at PT #3 the predicted flow depth was 4 cm lower than the observed depth, which was attributed to the impact of buildings on the local flow distribution.

Areas subject to flooding were classified as either Type A (due to insufficient hydraulic capacity of a sewer), Type B (which is an area without flooding notwithstanding insufficient hydraulic capacity of a sewer) or Type C (due to inlet limitations, i.e. there is hydraulic capacity in a sewer which is not utilized). In the total flooded zone, 24% was classified as Type A (10.2 ha) and 25% was classified as Type C (2.61 ha). It was concluded that greater attention should be paid to the area classified as Type B, which covers 50.5% (5.15 ha) of the total flooded zone.

It is also concluded that assessing the causes of flooding in an urban area using a 1D/2D model provides valuable information on the cause of flooding and is able to inform the planning of sewer rehabilitation to reduce the impacts of flooding on the local community.

ACKNOWLEDGEMENT

This research was supported by the National Research Foundation of Korea under the Korean government (Ministry of Education and Science Technology (MEST)) in 2012 (No. 2011-0028914).

REFERENCES

Aronica, G. T. & Lanza, L. G. 2005 Drainage efficiency in urban areas: a case study. *Hydrological Processes* **19**, 1105–1119.

Djordjevic, S., Prodanovic, D. & Makximovic, C. 1999 An approach to simulation of dual drainage. *Water Science and Technology* **39** (5), 95–103.

Fewtrell, T. J., Bates, P. D., Horritt, M. & Hunter, N. M. 2008 Evaluating the effect of scale in flood inundation modeling in urban environments. *Hydrological Processes* **22**, 5107–5118.

Lai, C. T. 1986 Numerical modeling on unsteady open-channel flow. In: *Advances in Hydroscience* (B. C. Yen, ed.). Academic Press, New York, pp. 189–250.

Leitao, J. P., Boonaya-aroonnet, S., Prodanovic, D. & Maksimovic, C. 2009 The influence of digital elevation model resolution on overland flow networks for modeling urban pluvial flooding. *Water Science and Technology* **60**, 3137–3149.

Meierdiercks, L. K., Smith, J. A., Baeck, M. L. & Miller, A. J. 2010 Analysis of urban drainage structure and its impact on hydrologic response. *Journal of the American Water Resources Association* **46**, 932–943.

Schubert, J. E., Sanders, B. F., Smith, M. J. & Wright, N. G. 2008 Unstructured mesh generation and landcover-based resistance for hydrodynamic modeling of urban flooding. *Advances in Water Resources* **31**, 1603–1621.

WBM Oceanics 2003 TUFLOW (and ESTRY) User Manual – GIS Based 2D/1D Hydrodynamic Modelling, User Manual, July, Brisbane.

First received 25 November 2013; accepted in revised form 28 January 2014. Available online 19 February 2014